Accepted Manuscript

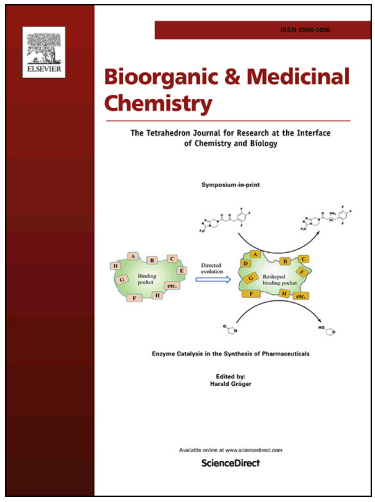

New pyrazolopyrimidine derivatives as *Leishmania amazonensis* arginase inhibitors

Livia M. Feitosa, Edson R. da Silva, Lucas V.B. Hoelz, Danielle L. Souza, Julio A.A.S.S. Come, Camila Cardoso-Santos, Marcos M. Batista, Maria de Nazare C. Soeiro, Nubia Boechat, Luiz C.S. Pinheiro

PII: S0968-0896(19)30475-4
DOI: https://doi.org/10.1016/j.bmc.2019.05.026
Reference: BMC 14913

To appear in: *Bioorganic & Medicinal Chemistry*

Received Date: 22 March 2019
Revised Date: 10 May 2019
Accepted Date: 16 May 2019

Please cite this article as: Feitosa, L.M., da Silva, E.R., Hoelz, L.V.B., Souza, D.L., Come, J.A.A., Cardoso-Santos, C., Batista, M.M., Soeiro, d.N.C., Boechat, N., Pinheiro, L.C.S., New pyrazolopyrimidine derivatives as *Leishmania amazonensis* arginase inhibitors, *Bioorganic & Medicinal Chemistry* (2019), doi: https://doi.org/10.1016/j.bmc.2019.05.026

Bioorganic & Medicinal Chemistry
journal homepage: www.elsevier.com

New pyrazolopyrimidine derivatives as *Leishmania amazonensis* arginase inhibitors

Livia M. Feitosa[a,b] , Edson R. da Silva[c,*] , Lucas V. B. Hoelz[a] , Danielle L. Souza[a] , Julio A. A. S. S. Come[d] , Camila Cardoso-Santos[e] , Marcos M. Batista[e] , Maria de Nazare C. Soeiro[e] , Nubia Boechat[a,] * and Luiz C. S. Pinheiro[a]

[a]*Departamento de Sintese de Farmacos, Instituto de Tecnologia em Farmacos, Farmanguinhos - FIOCRUZ, Fundação Oswaldo Cruz. Rua Sizenando Nabuco 100, Manguinhos, Rio de Janeiro, RJ, 21041-250, Brazil.*
[b]*Programa de Pos-graduacao em Quimica, PGQu Instituto de Quimica, Universidade Federal do Rio de Janeiro, Rio de Janeiro, RJ, Brazil.*
[c]*Departamento de Medicina Veterinaria, Faculdade de Zootecnia e Engenharia de Alimentos, Universidade de Sao Paulo, Pirassununga, SP, Brazil.*
[d]*Programa de Pos-graduacao em Biociencia Animal, Faculdade de Zootecnia e Engenahria de alimentos, Universidade de São Paulo, Pirassununga, SP, Brazil.*
[e]*Laboratorio de Biologia Celular, Instituto Oswaldo Cruz, IOC - FIOCRUZ, Fundacao Oswaldo Cruz. Avenida Brasil 4365, Rio de Janeiro, RJ, Brazil.*

ARTICLE INFO

Article history:
Received
Received in revised form
Accepted
Available online

Keywords:
Leishmania amazonensis
pyrazolopyrimidine
arginase
trypanothione
polyamines

ABSTRACT

Arginase performs the first enzymatic step in polyamine biosynthesis in *Leishmania* and represents a promising target for drug development. Polyamines in *Leishmania* are involved in trypanothione synthesis, which neutralize the oxidative burst of reactive oxygen species (ROS) and nitric oxide (NO) that are produced by host macrophages to kill the parasite. In an attempt to synthesize arginase inhibitors, six 1-phenyl-1*H*-pyrazolo[3,4-*d*]pyrimidine derivatives with different substituents at the 4-position of the phenyl group were synthesized. All compounds were initially tested at 100 μM concentration against *Leishmania amazonensis* ARG (*La*ARG), showing inhibitory activity ranging from 36 to 74%. Two compounds, **1** (R = H) and **6** (R = CF_3), showed arginase inhibition >70% and IC_{50} values of 12 μM and 47 μM, respectively. Thus, the kinetics of *La*ARG inhibition were analyzed for compounds **1** and **6** and revealed that these compounds inhibit the enzyme by an uncompetitive mechanism, showing K_{is} values, and dissociation constants for ternary complex enzyme-substrate-inhibitor, of 8.5 ± 0.9 μM and 29 ± 5 μM, respectively. Additionally, the molecular docking studies proposed that these two uncompetitive inhibitors interact with different *La*ARG binding sites, where compound **1** forms more H-bond interactions with the enzyme than compound **6**. These compounds showed low activity against *L. amazonensis* free amastigotes obtained from mice lesions when assayed with as much as 30 μM. The maximum growth inhibition reached was between 20-30% after 48 h of incubation. These results suggest that this system can be promising for the design of potential antileishmanial compounds.

* Corresponding author. Tel.: +55-21-3977-2456; e-mail: nubia.boechat@far.fiocruz.br (N.B.); e-mail: edsilva@usp.br (E.R.S.)

1. Introduction

Leishmaniasis is caused by different species of the genus *Leishmania*, which produce a variety of clinical diseases that affect mainly humans and dogs. Visceral leishmaniasis (kala-azar) leads to more than 20,000 deaths reported annually, while cutaneous leishmaniasis has affected 1 million people in the last 5 years. The World Health Organization estimates that 310 million people are at risk of contracting the infection in the six countries that showed 90% of the kala-azar cases.[1] The drug treatment is mainly based on pentavalent antimonials and amphotericin B, both which carry high host toxicity.[2-4]

Leishmania arginase catalyzes the conversion of L-arginine into L-ornithine and urea in the first step of polyamine biosynthesis. Polyamines are essential for parasites to synthesize trypanothione, an antioxidant compound produced by trypanosomatids, that is able to neutralize the reactive oxygen species (ROS) and reactive nitric oxide (NO) produced by host macrophages to control the infection.[5-7] The structural differences in *Leishmania* arginase and human liver arginase described for *Leishmania amazonensis* (*La*ARG)[8] and *Leishmania mexicana*[9] opened a new path to selective drug design to treat leishmaniasis.

The natural compound Nω-hydroxy-L-arginine inhibits arginase of both the parasite and host, showing activity against the *Leishmania* infection.[10,11] Nonselective synthetic inhibitors designed to target mammalian arginase[12,13] showed similar competitive inhibition of *La*ARG, and the X-ray structure of the parasitic *La*ARG revealed differences in their tridimensional structure, which could be exploited for drug development.[11]

Previously, we demonstrated the importance of [1,2,4]triazolo[1,5-*a*]pyrimidine derivatives as antimalarial compounds, which were planned as bioisosteres of chloroquine[14]. As triazolopyrimidine is a bioisostere of the arginase inhibitor chloroquine and arginase is a potential target for leishmaniasis, we decided to test the series of [1,2,4]triazolo[1,5-*a*]pyrimidine derivatives. The literature has described that compounds **I-IV**, presenting structural units such as N(C=N)N, N(C=S)N, or C(C=N)N (**Figure 1**), showed leishmanicidal activity[15]. The results of our work confirm that the introduction of a thiosemicarbazide structural unit at the 7-position of the [1,2,4]triazolo[1,5-*a*]pyrimidine ring increased *La*ARG enzyme inhibition[16]. 2-(5-Methyl-2-(trifluoromethyl)-[1,2,4]triazolo[1,5-*a*]pyrimidin-7-yl)hydrazinecarbothioamide (Compound **V**) was the most potent, inhibiting *La*ARG by a noncompetitive mechanism with a K_i = 17 μM and IC_{50} = 16.5 μM.[16]

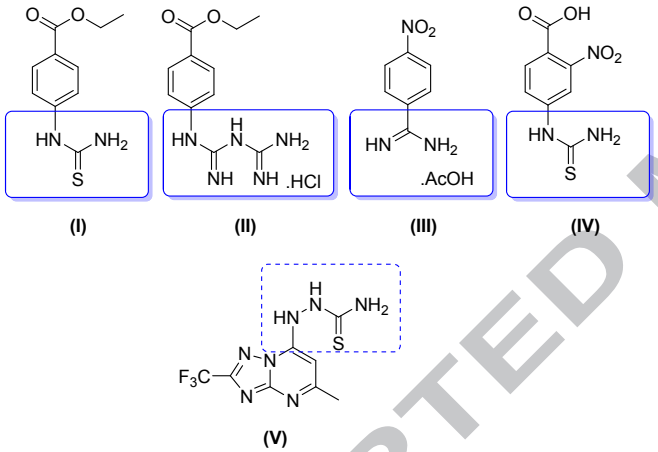

Figure 1. Structures of compounds **I-V** which have the structural units (blue) present in anti-leishmanial substances.

To find new compounds with antileishmanial activity, we used compound **V** as a prototype to develop new derivatives, the 2-(1-phenyl-1*H*-pyrazolo[3,4-*d*]pyrimidin-4-yl)hydrazinecarbothioamides (**1-6**). These compounds were designed based on the ring bioisosterism replacing the triazolo[1,5-*a*]pyrimidine system (green) with a 1-phenyl-1*H*-pyrazolo[3,4-*d*]pyrimidine system (red) (**Figure 2**). The thiosemicarbazide subunit (blue) also present in **V** is known as a pharmacophoric group for antileishmanial activity and was attached at the 4-position of the heterocyclic ring, similar to what was found in the individual molecular framework of the prototype **V** (**Figure 2**). The antileishmanial activities, cytotoxicity and inhibition of *La*ARG by the [1,2,4]triazolo[1,5-*a*]pyrimidine and 1*H*-pyrazolo[3,4-*d*]pyrimidine systems were then determined.

2. Results and discussion

2.1. Chemistry

The synthetic route for preparing the 2-(1-phenyl-1*H*-pyrazolo[3,4-*d*]pyrimidin-4-yl)hydrazinecarbothioamides **(1-6)** is shown in **Scheme 1**. The 5-amino-1-phenyl-1*H*-pyrazole-4-carbonitriles **(7-12)** could be prepared in 48-90% yield from the reaction of the appropriate phenylhydrazine and 2-(ethoxymethylene)malononitrile in ethanol under reflux for 2 h.[17] The 1-phenyl-1*H*-pyrazolo[3,4-*d*]pyrimidin-4(5*H*)-ones **(13-18)** could be prepared in 68-89% yield from the reaction of the suitable 5-amino-1-phenyl-1*H*-pyrazole-4-carbonitriles **(7-12)** and formic acid under reflux for 12 h.[18] The derivatives **(13-18)** were refluxed with phosphorous oxychloride for 24 h to produce 4-chloro-1-phenyl-1*H*-pyrazolo[3,4-*d*]pyrimidines **(19-24)** in 78-97% yield.[19-20]

The compounds 2-(1-phenyl-1*H*-pyrazolo[3,4-*d*]pyrimidin-4-yl)hydrazinecarbothioamides (**1-6**) were obtained by the nucleophilic substitution reaction between the appropriate 4-chloro-1-phenyl-1*H*-pyrazolo[3,4-*d*]pyrimidine derivatives **(19-24)** and thiosemicarbazide in DMF at 25 °C for 24 h in 23-50% yield.[16]

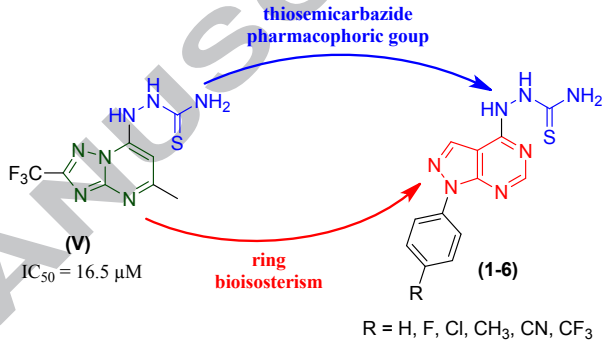

Figure 2. Rational approach to the design of compounds **1-6** based on the ring bioisosterism replacing the triazolo[1,5-*a*]pyrimidine system (green) by a 1-phenyl-1*H*-pyrazolo[3,4-*d*]pyrimidine system (red).

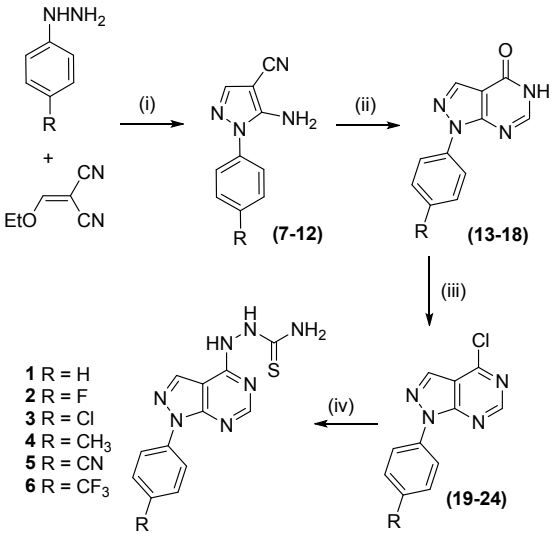

Reagents and conditions: (i) EtOH, reflux, 2 h, 48-90%; (ii) HCOOH, reflux, 12 h, 68-89%; (iii) $POCl_3$, reflux, 24 h, 78-97%; (iv) thiosemicarbazide, DMF, 25 °C, 24 h 23-50%.

Scheme 1. Synthetic route used to prepare compounds **1-6**.

Table 1.
Arginase inhibition by 1-phenyl-1*H*-pyrazolo[3,4-*d*]pyrimidines (**1-6**).

Compounds	Arginase inhibition			
	100 µM (%)	IC_{50} (µM) (CI)[a]	K_{is} (µM)[b]	Mechanism
1 R = H	74.3	12 (8.544 – 18.03)	8.5 ± 0.9	uncompetitive
2 R = F	36.4	>100	[c]ND	ND
3 R = Cl	46.0	>100	ND	ND
4 R = CH_3	42.2	>100	ND	ND
5 R = CN	59.8	~100	ND	ND
6 R = CF_3	73.8	47 (37.12 – 75.83)	29 ± 5	uncompetitive
Prototype **V**	81.0	16.5	17 ± 1	noncompetitive

[a]CI = 95% confidence interval; [b] Standard error of mean; [c] ND = not determined. IC_{50}: data performed at 50 mM of substrate.

2.2. Determination of IC_{50} values and Kinetics of *L. amazonensis* arginase inhibition

All compounds were initially tested at 100 µM against recombinant *L. amazonensis* arginase (*La*ARG) to verify inhibition of the enzyme, and the results are presented in **Table 1**. Compounds **1** (R = H) and **6** (R = CF_3) show an inhibition of approximately 74%, while the other compounds showed a weak inhibition (36-59%). The concentration that inhibits 50% of the enzyme activity (IC_{50}) was determined for compounds **1** and **6** using three L-arginine concentrations: 25, 50 and 100 mM. The data showed that the IC_{50} values did not differ statistically ($p>0.05$) when the concentration of the substrate L-arginine was increased (**Figure 3**), indicating that **1** and **6** were not competitive inhibitors of *La*ARG.

Compounds **1** and **6** showed IC_{50} values of 12 µM and 47 µM, respectively. The IC_{50} value shown in **Table 1** is the result performed at 50 mM L-arginine used previously to test prototype **V**.[16]

Then, the kinetic characterization of LaARG inhibition was performed on **1** and **6** and the analysis of the Dixon and Cornish-Bowden plots (**Figure 4**) indicate that both showed an uncompetitive mechanism of enzyme inhibition; this shows that they simultaneously bind substrate L-arginine and inhibitor in a ternary ESI complex (enzyme-substrate-inhibitor) as predicted by the Michaelis-Menten equation model of enzyme inhibition. Compound **1** (R = H) showed a K_{is} = 8.5 ± 0.9 µM while **6** (R = CF_3) had a K_{is} = 29 ± 5 µM (**Table 1**).

Compound **1** (R = H), which had estimated K_i and IC_{50} values for *La*ARG of 8.5 µM and 12 µM, respectively, proved to be 1.5-2-fold more potent than the prototype **V** (K_i = 17 µM, IC_{50} = 16.5 µM). Compound **6** (R_1 = CF_3) exhibited K_i and IC_{50} values of 29 µM and 47 µM, respectively; however, the precursor was still more potent than this derivative (**Table 1**).

2.3. Macrophage cytotoxicity and antileishmanial activity

The cytotoxicities of compounds **1**, **2**, **3**, **6**, and prototype **V** were tested against mouse peritoneal macrophages that were incubated for 48 h with increasing concentrations of the five molecules. Our findings demonstrated that all compounds did not show toxicity on mammalian cells, exhibiting LC_{50} values > 200 µM. When these compounds were tested against amastigotes of *L. amazonensis* purified from mouse skin lesions, we found that all presented weak leishmanicidal potency when assessing to a concentration of 30 µM, reaching maximum parasite death rates of 20-30% against free amastigotes. Pentamidine showed an EC_{50} value of 0.8 µM, although it also displayed high host cell toxicity (LC_{50} of 17.2 µM). Compounds **4** and **5** precipitated out in concentrations higher than 25 µM, and their cytotoxicity was not

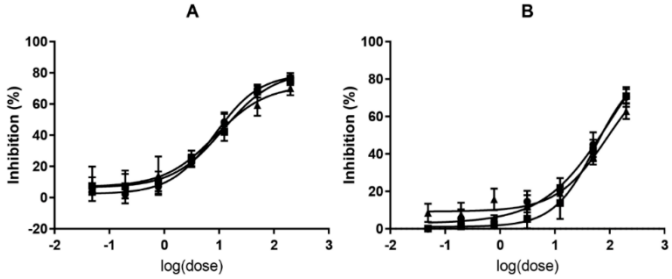

Figure 3. Dose-response curve of arginase inhibition by compound **1** (A) and **6** (B). Inhibitor concentrations: 0.05-200 µM. The concentrations of L-Arginine used were 100 mM (●), 50 mM (■) and 25 mM (▲).

2.4. Molecular Modeling

2.4.1. Comparative Modeling

To gain insights into the complex between these uncompetitive inhibitors and *La*ARG, we built a 3D model of this enzyme in the monomeric and trimeric forms (potential arrangements found in biological medium), since a high-quality model was not available in the PDB. Thus, the *La*ARG models showed good structural quality when evaluated by PROCHECK[21] and VERIFY3D[22] (**Figures S1-4**).

In addition, the *La*ARG models encompass an active site that lies at the bottom of a 15 Å deep cleft. Two essential Mn^{2+} ions are located at the bottom of this cleft, separated by approximately 3.3 Å, and bridged by the carboxylate groups from two aspartic acid residues and interacting with the arginine substrate.[23-24]

These models also present an overall fold formed by a parallel 8 stranded β-sheet flanked on both sides by numerous α-helices, as described for other Leishmania arginase structures.[11,24,25]

2.4.2. Molecular docking

To compare the binding modes of the two inhibitors **1** and **6** and prototype **V** to the *La*ARG models, we carried out five molecular docking simulations for each ligand (totaling 50 poses per ligand) and, consequently, the poses with the lowest energy were selected for analysis. The comparison between the poses of each inhibitor is represented in **Figure 5**.

The molecular docking study showed that inhibitors **1** and **6** have different interaction modes and energy interaction values with both forms of the *La*ARG model (**Figure 5** and **Table 2**). Inhibitor **1** presents MolDock score values of -104.16 a.u. and -115.21 a.u., while inhibitor **6** shows values of -112.61 a.u. and -125.06 a.u. in the monomeric and the trimeric forms, respectively. In addition, the hydrogen bonds (H-bonds) and steric interactions were mapped using a ligand-map algorithm, generated by the MVD program.[26] The H-bonds are represented in **Figure 5**.

Considering the monomeric *La*ARG model, inhibitor **1** interacts via H-bonds with Glu167, Ile169, Glu171 and Ser174 (H-bond energy = -5.57 a.u.; **Figure 5C-D**), and presents steric interactions with Arg166, Glu167, Ile169, Glu171, Ser174, Val176, and Gln178 (steric interaction energy = -15.95 a.u.) (**Table 2**). Inhibitor **6** forms H-bonds with Leu190 and Arg191 (H-bond energy = -4.52 a.u.; **Figure 5E-F**) and shows steric interactions with Leu190, Arg191, Val193, Leu201, His202, Arg205, Ile206, and Ser210 (steric interaction energy = -21.08 a.u.) (**Table 2**).

In the trimeric *La*ARG model, inhibitor **1** binds at the interface between the A chain and B chain, making H-bonds and steric interactions with Arg191, Asp215, Arg266, and Glu273 (H-bond energy = -5.46 a.u. and steric interaction energy = -40.17 a.u.) (**Table 2**). The amino acid residues Asp215, Arg266 and Glu273 are involved in H-bond interactions with the trimeric arginase of *Leishmania mexicana*.[11] In rat liver-type arginase, there is a decrease in activity with a single R308K mutation in the monomeric form,[27] and in *La*ARG the disruption of the trimeric form by **1** can be responsible for its uncompetitive inhibition of the enzyme. Differently, inhibitor **6** binds between chains B and C, making H-bonds with Pro258 and Arg260 and steric interactions with Asp 215, Pro258, and Arg260 (steric interaction energy = -37.81 a.u.).

Additionally, the molecular docking study showed that prototype **V** presents MolDock score values of -91.66 a.u. and -115.37 a.u. in the monomeric and the trimeric forms, respectively (**Table 2**). This inhibitor interacts with the *La*ARG model within the same cavity as inhibitor **1** (**Figure 5A**) in the monomeric form, via H-bond interactions with Lys198 (H-bond energy = -3.31 a.u.; **Figure 5G-H**), and presents steric interactions with Lys198, Leu201, Asn205, and Ile206 (steric interaction energy = -18.91 a.u.). In the trimeric *La*ARG model, prototype **V** binds at the interface between chains A and B, making H-bonds with Arg191, Ser210, and Glu273. This inhibitor also makes steric interactions with Arg191, Ser210, His212, Asp215, and Glu273 (H-bond energy = -6.53 a.u. and steric interaction energy = -30.98 a.u.) (**Table 2**).

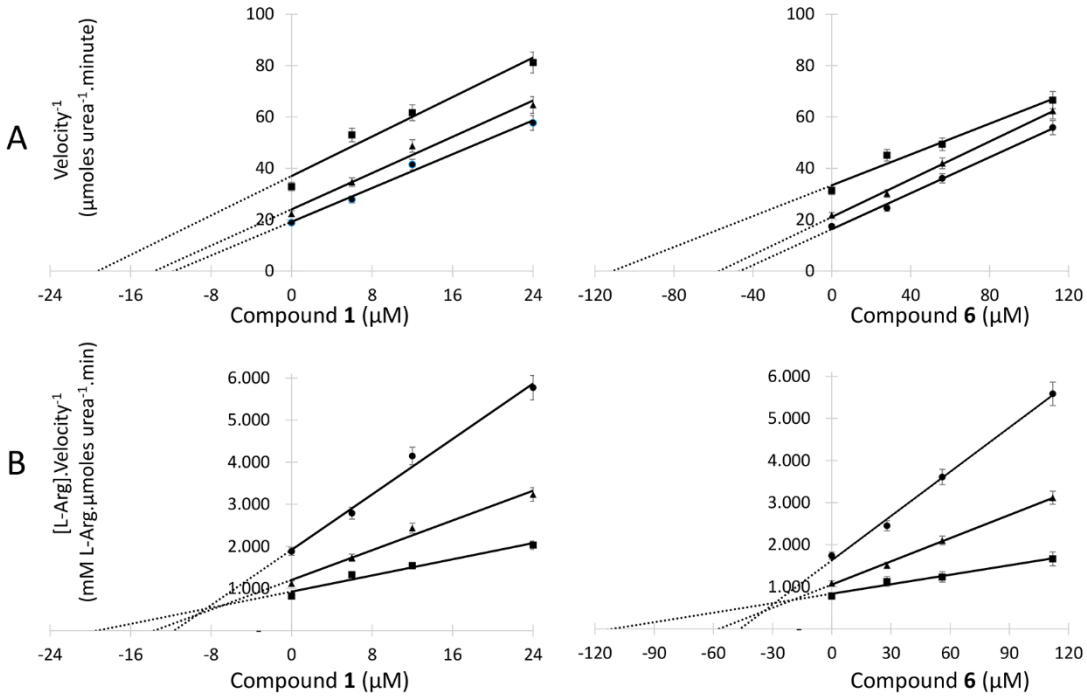

Figure 4. Kinetics of arginase inhibition by **1** and **6**. The mechanisms of action were determined by analysis of the Dixon (A) and Cornish-Bowden plots (B) and the K_{is} constant was measured using the Cornish-Bowden plot (B). The concentrations of L-arginine used were 100 mM (●), 50 mM (▲) and 25 mM (■). The inhibitor concentrations used were 6, 12 and 24 µM for compound **1**, and 28, 56 and 112 µM for compound **2**. Each point drawn represents the mean of three independent experiments (n = 3) performed in duplicate.

Table 2.
Summary of the interactions of each inhibitor with the *L. amazonensis* arginase model in monomeric and trimeric forms.

Monomeric Form					
Inhibitors	H-bond energy (a.u.)[a]	Residues (H-bond interaction)	Steric interaction energy by PLP [b] (a.u.)	Residues (steric interactions)	MolDock score (a.u.)
1	-5.57	Glu167, Ile169, Glu171, Ser174	-15.95	Arg166, Glu167, Ile169, Glu171, Ser174, Val176, Gln178	-104.16
6	-4.52	Leu190, Arg191	-21.08	Leu190, Arg191, Val193, Leu201, His202, Arg205, Ile206, Ser210	-112.61
Prototype **V**	-3.11	Lys198	-18.91	Lys198, Leu201, Asn205, Ile206	-91.66
Trimeric Form					
Inhibitors	H-bond energy (a.u.)	Residues (H-bond interaction)	Steric interaction energy by PLP (a.u.)	Residues (steric interactions)	MolDock score (a.u.)
1	-5.46	Arg191(A)[c], Asp215(A), Arg266(C), Glu273(C)	-40.17	Arg191(A), Asp215(A), Arg266(C), Glu273(C)	-115.21
6	-3.98	Pro258(C), Arg260(C)	-37.81	Asp215(B), Pro258(C), Arg260(C)	-125.06
Prototype **V**	-6.53	Arg191(B), Ser210(B), Glu273(A)	-30.98	Arg191(B), Ser210(B), His212(B), Asp215(B), Glu273(A)	-115.37

[a] Arbitrary units; [b] Piecewise linear potential; [c] The letter within the parenthesis indicates the chain of the respective residue.

3. Results and discussion

Previously, we described the new synthetic prototype **V**, containing a thiosemicarbazide as a pharmacophoric group, which was used as our prototype for this study.[16] Six 1-phenyl-1*H*-pyrazolo[3,4-*d*]pyrimidine derivatives (**1**-**6**) containing thiosemicarbazide as the pharmacophoric group were synthesized with different substituents in the 4-position of the phenyl subunit. The compounds were tested for *La*ARG inhibition, antileishmanial activity and cytotoxicity. Compounds **1** (R = H) and **6** ($R_1 = CF_3$) showed *La*ARG inhibition with IC_{50} values of 12 and 47 μM, respectively. The kinetics study with *La*ARG showed that **1** and **6** are both uncompetitive inhibitors with K_{is} values of 8.5 ± 0.9 μM and 29 ± 5 μM, respectively. The data of the kinetics study showed that compound **1** (R = H) was 1.5-fold more potent than prototype **V** (K_i = 17 ± 1 μM) against *La*ARG. This result suggests that the ring exchange proposed in this work can change the mechanism of *La*ARG inhibition from noncompetitive (prototype **V**) to uncompetitive (compounds **1** and **6**), where compound **1** (R= H) was a more potent inhibitor than compound **6** (R= CF_3), presenting lower IC_{50} and K_i values. In addition, compounds **2** (R= F), **3** (R= Cl), and **4** ($R_1 = CH_3$) showed decreased *La*ARG inhibition. Compound **5** (R= CN) caused a minor effect on *La*ARG inhibition. The whole-cell assays using these inhibitors showed that all compounds were not toxic to the mammalian host cells, exhibiting LC_{50} values higher than 200 μM, while the LD_{50} of pentamidine is at least 10-fold higher (17 μM) on peritoneal macrophages. However, those compounds were also not toxic to the parasite, since none were able to induce more than 10% parasitic death when assayed using 30 μM for 48 h of incubation. The data stimulates compound optimization to improve the potency against these parasites, which causes cutaneous leishmaniasis.

Interestingly, the molecular docking analysis drives freely outside of the active site, to an allosteric site. In the monomeric form of the *La*ARG model, compound **1** (R = H) and prototype **V** interacted with the same cavity, in a different way than compound **6** (R= CF_3). However, the docking of compound **1** (R = H) and prototype **V** in the trimeric form of the enzyme model propose binding sites in pockets between the A and C chains and A and B chains, respectively, while compound **6** (R= CF_3) seems to interact in a cavity formed between the B and C chains. These three inhibitors interact with arginase models through H-Bonds and steric interactions, where the number of interactions that each compound makes in the trimeric form of the *La*ARG model seems to be important for inhibitory activity (**Table 2**, **Figure 5**). Thus, compound **1** (R = H) makes more interactions with the enzyme, presenting the lower IC_{50} value, followed by prototype **V** and compound **6** (R= CF_3). Additionally, these docking insights are in agreement with the kinetics of *La*ARG inhibition.

The arginase enzyme is located in a unique trypanosomatidae organelle known as the glycosome.[28] To deliver the drug that targets arginase in intracellular amastigotes it must be absorbed by a macrophage, enter the peroxisome, reach the *Leishmania* cytosol, and be delivered to the glycosome compartment to block the enzyme. This biological barrier may explain the absence of activity against intracellular amastigotes of *L. amazonensis*.

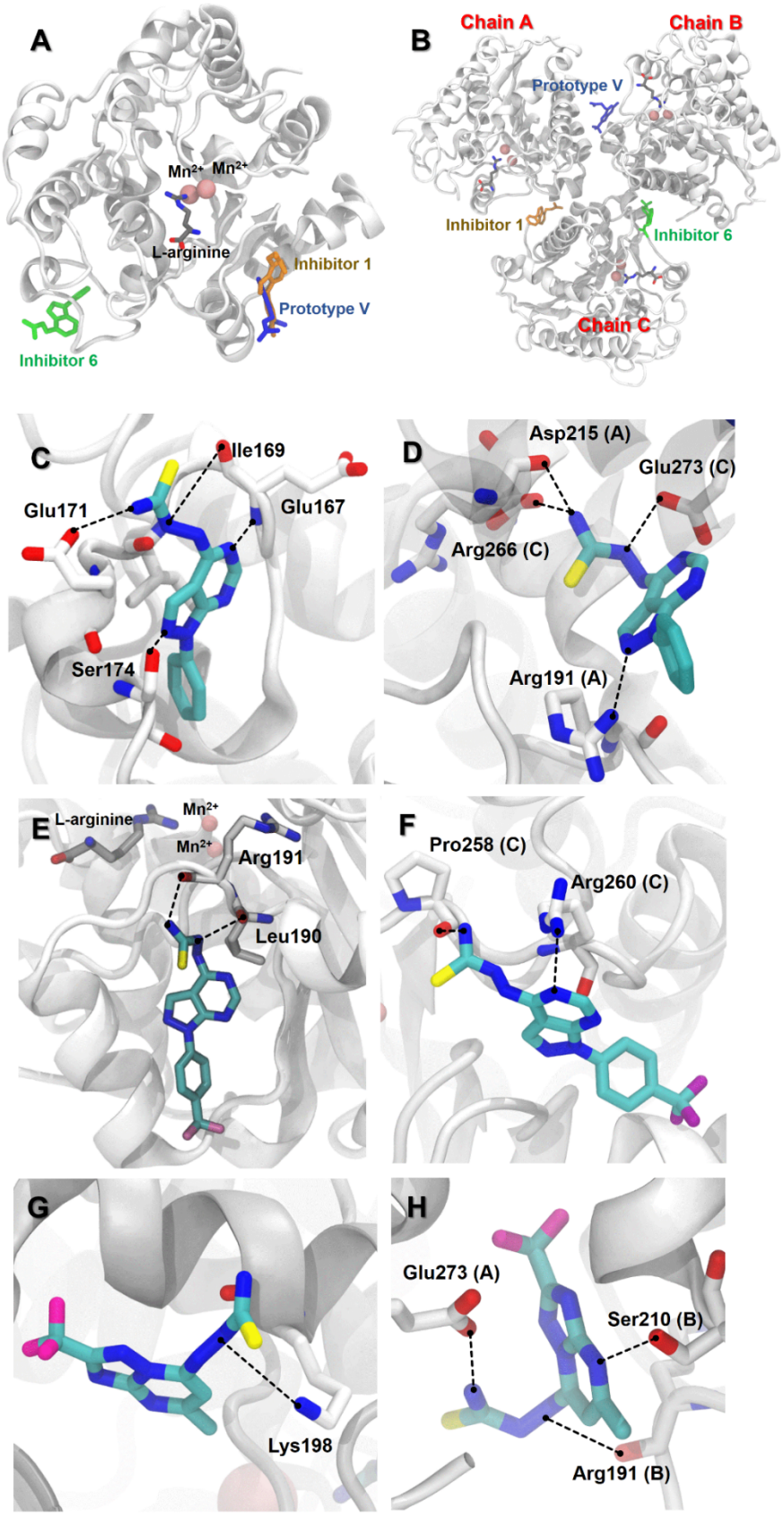

Figure 5. Cartoon structural representation of the arginase (*La*ARG) models, in monomeric (**A**) and trimeric (**B**) forms, in complex with the uncompetitive inhibitors **1** and **6** and prototype **V**. Representation of H-bond interactions in each complex: **1** (**C**), **6** (**E**), and prototype **V** (**G**) in monomeric form, and **1** (**D**), **6** (**F**), and prototype **V** (**H**) in trimeric form, showing the respective chain within the parenthesis. The H-bonds are represented by black interrupted lines. The inhibitors and *La*ARG residue structures are in stick model and colored by atom: the nitrogen atoms are shown in blue, the oxygen atoms in red, the fluorine atoms in purple, and the carbon chain in white or cyan.

4. Conclusions

Among the 1-phenyl-1*H*-pyrazolo[3,4-*d*]pyrimidines (**1-6**) synthesized with different substituents at the 4-position of the phenyl group, compounds **1** (R = H) and **6** (R_1 = CF_3) exhibited *La*ARG inhibition. However, the best performance was observed for compound **1** (R = H), which had K_i and IC_{50} values estimated to be 8.5 μM and 12 μM, respectively, proving to be 1.5-fold more potent than prototype **V**. All tested compound were not toxic *in vitro* on mouse peritoneal cells, but unfortunately they were not active against amastigotes purified from animal lesions. Additionally, the molecular docking studies propose that these two uncompetitive inhibitors interact with different *La*ARG binding sites, where compound **1** (R = H) forms more H-bond interactions with the enzyme than compound **6** (R= CF_3). Therefore, the 1*H*-pyrazolo[3,4-*d*]pyrimidine system seems to be a promising prototype for further studies of antileishmanial candidates based on *La*ARG inhibition. The weak action on *L. amazonensis* amastigotes can be due to the relatively low hydrophobicity that decreases the bioavailability into the parasite and blocks *La*ARG. These results indicate that the hydrophobicity of the phenyl moiety of **1** (R = H) is important to design *La*ARG inhibitors with the 1-phenyl-1*H*-pyrazolo[3,4-*d*]pyrimidine scaffold, and a study of a delivery system can be performed for *La*ARG inhibition *in vivo*. These results suggest that this system can be promising for the design of potential antileishmanial compounds.

5. Materials and Methods

5.1. Chemistry

All reagents and solvents used were of analytical grade. The ^{1}H, ^{13}C and ^{19}F nuclear magnetic resonance (NMR) spectra were obtained at 400.00, 100.00 and 376.00 MHz, respectively, using a BRUKER Avance instrument equipped with a 5 mm probe. Tetramethylsilane was used as an internal standard. The chemical shifts (δ) are reported in ppm, and the coupling constants (J) are reported in Hertz. Electron-ionization mass spectra (EI-MS, scan ES+ capillary (3.0 kV)/cone (30 V)/extractor (1 V)/RF lens (1.0 V)/source temperature (150 °C)/desolvation temperature (300 °C)) were recorded using a Micromass/Waters Spectrometer (model: ZQ-4000). High Resolution Mass Spectrometry (HRMS) data were obtained using an LC-MS Bruker Daltonics MicroTOF (time of flight analyzer). Fourier transform infrared (FT-IR) absorption spectra were recorded on a Shimadzu mode IR Prestige-21 spectrophotometer through KBr reflectance. The melting points (m.p.) were determined using a Büchi model B-545 apparatus. TLC (thin layer chromatography) was performed using a silica gel F-254 glass plate (20 × 20 cm).

5.1.1. General procedure for preparing 5-amino-1-phenyl-1*H*-pyrazole-4-carbonitriles (7-12)

A mixture of the appropriate phenylhydrazine (0.001 mol) and 10 mL of ethanol was stirred and allowed to reflux. Then, 2-(ethoxymethylene)malononitrile (0.001 mol) dissolved in 10 mL of ethanol was slowly added. The reaction mixture was refluxed for 2 h. The reaction mixture was poured into 50 mL of ice-cold water. The precipitate was collected by filtration and washed with water to produce **7-12** in 48-90% yield.

5-amino-1-phenyl-1*H*-pyrazole-4-carbonitrile **(7)**. Yield: 90%. MP: 135-136 °C. IR (cm^{-1}): 3222-3193; 3052; 2220; 1637; 1599. ^{1}H NMR (400 MHz, DMSO-d_6, TMS, δ in ppm): 6.68 (s; 2H; NH_2); 7.55-7.49 (m; 4H; H2', H3', H5', H6'); 7.45-7.40 (m; 1H; H4'); 7.78 (s; 1H; H3). ^{13}C NMR (100 MHz, DMSO-d_6, TMS, δ in ppm): 73.3 (C4); 114.8 (CN); 124.1 (C2', C6'); 127.8 (C4'); 129.4 (C3', C5'); 137.4 (C1'); 141.7 (C5); 151.2 (C3). ^{19}F NMR (376 MHz, DMSO-d_6, TMS, δ in ppm): -114.26. EI $[M+1]^+$ 185.07.

5-amino-1-(4-fluorophenyl)-1*H*-pyrazole-4-carbonitrile **(8)**. Yield: 61%. MP: 173-174 °C. IR (cm^{-1}): 3297-3183; 2225; 1662; 1568; 1222. ^{1}H NMR (400 MHz, DMSO-d_6, TMS, δ in ppm): 7.31-7.25; (m; 2H; H3', H5'); 7.54-7.49; (m; 2H; H2', H6'); 7.67; (s; 1H; H3). ^{13}C NMR (100 MHz, DMSO-d_6, TMS, δ in ppm): 73.2 (C4); 114.8 (CN); 116.3 (d; J = 22.8 Hz; C3', C5'); 126.9 (d; J = 8.9 Hz; C2', C6'); 133.7 (d; J = 2.8 Hz; C1') 141.7 (C5); 151.4 (C3); 161.2 (d; J = 243.6 Hz; C4'). ^{19}F NMR (376 MHz, DMSO-d_6, TMS, δ in ppm): -114.26. EI $[M+1]^+$ 203.07.

5-amino-1-(4-chlorophenyl)-1*H*-pyrazole-4-carbonitrile **(9)**. Yield: 78%. MP: 164-166 °C. IR (cm^{-1}): 3295-3174; 2229; 1663; 1562; 828. ^{1}H NMR (400 MHz, DMSO-d_6, TMS, δ in ppm): 7.50; (d; 2H; J = 8.9 Hz H3', H5'); 7.55; (d; 2H; J = 8.9 Hz; H2', H6'); 7.68; (s; 1H; H3). ^{13}C NMR (100 MHz, DMSO-d_6, TMS, δ in ppm): 73.5 (C4); 114.6 (CN); 126.0 (C2', C6'); 129.4 (C3', C5'); 132.2 (C4') 136.3 (C1'); 142.0 (C5); 151.4 (C3). EI $[M+1]^+$ 219.07.

5-amino-1-(*p*-tolyl)-1*H*-pyrazole-4-carbonitrile **(10)**. Yield: 80%. MP: 147-149 °C. IR (cm^{-1}): 3357-3314; 2214; 1660; 1564. ^{1}H NMR (400 MHz, DMSO-d_6, TMS, δ in ppm): 2.36 (s; 3H; CH_3); 6.60 (s; 2H; NH_2); 7.32; (d; 2H; J = 8.9 Hz; H2', H6'); 7.36; (d; 2H; J = 8.9 Hz; H3', H5'); 7.75; (s; 1H; H3). ^{13}C NMR (100 MHz, DMSO-d_6, TMS, δ in ppm): 73.2 (C4); 114.8 (CN); 124.1 (C2', C6'); 129.8 (C3', C5'); 134.9 (C4') 137.4 (C1'); 141.4 (C5); 151.1 (C3). EI $[M+1]^+$ 199.09.

5-amino-1-(4-cyanophenyl)-1*H*-pyrazole-4-carbonitrile **(11)**. Yield: 57%. MP: 187-189 °C. IR (cm^{-1}): 3377-3341; 2224; 2192; 1606; 1560. ^{1}H NMR (400 MHz, DMSO-d_6, TMS, δ in ppm): 6.97 (s; 2H; NH_2); 7.75 (d; 2H; J = 8.8 Hz; H3', H5'); 7.88 (s; 1H; H3); 8.00 (d; 2H; J = 8.8 Hz; H 2', H6'). ^{13}C NMR (100 MHz, DMSO-d_6, TMS, δ in ppm): 74.0 (C4); 109.8 (C4'); 114.3 (CN); 118.2 (CN'); 124.1 (C2', C6') 133.6 (C3', C5'); 141.1 (C1'); 142.7 (C5); 151.6 (C3). EI $[M-1]^-$ 208.05.

5-amino-1-(4-(trifluoromethyl)phenyl)-1*H*-pyrazole-4-carbonitrile **(12)**. Yield: 48%. MP: 151-154 °C. IR (cm^{-1}): 3460-3139; 2213; 1614; 1563; 1315. ^{1}H NMR (400 MHz, DMSO-d_6, TMS, δ in ppm): 6.92 (s; 2H; NH_2); 7.76 (d; 2H; J = 8.0 Hz; H3', H5'); 7.91 (d; 2H; J = 8.0 Hz; H2', H6'); 7.86 (s; 1H; H3). ^{13}C NMR (100 MHz, DMSO-d_6, TMS, δ in ppm): 73.9 (C4); 114.5 (CN); 123.9 (q; J = 270.6 Hz; CF_3); 124.3 (C2', C6'); 126.6 (q; J = 3.8 Hz; C3', C5'); 127,7 (q; J = 32.0 Hz; C4'); 140.8 (C1'); 142.5 (C5); 151.6 (C3). ^{19}F NMR (376 MHz, DMSO-d_6, TMS, δ in ppm): -60.95. EI $[M-1]^-$ 251.31.

5.1.2. General procedure for preparing 1-phenyl-1*H*-pyrazolo[3,4-*d*]pyrimidin-4(5*H*)-ones (13-18)

A mixture of 5-amino-1-phenyl-1*H*-pyrazole-4-carbonitriles (**7-12**) (0.01 mol) and 20 mL of formic acid was stirred and allowed to reflux for 12 h. The reaction mixture was poured into 50 mL of ice-cold water. The precipitate was collected by filtration and washed with water to produce **13-18** in 68-89% yield.

1-phenyl-1*H*-pyrazolo[3,4-*d*]pyrimidin-4(5*H*)-one **(13)**. Yield: 74%. MP: > 300 °C. IR (cm^{-1}): 3116; 1727; 1660; 1591. ^{1}H NMR (400 MHz, DMSO-d_6, TMS, δ in ppm): 8.06-7.39 (m; 5H; HAr); 8.20 (d; 1H; J = 3.8 Hz; H6); 8.34 (s; 1H; H3); 12.46 (s; 1H; NH). ^{13}C NMR (100 MHz, DMSO-d_6, TMS, δ in ppm): 107.6 (C3a); 121.7 (C2', C6'); 127.1 (C4'); 129.1 (C3', C5'); 135.9 (C3); 138.2 (C1'); 148.7 (C6); 151.8 (C7a); 157.2 (C4). EI $[M+1]^+$ 213.07.

1-(4-fluorophenyl)-1*H*-pyrazolo[3,4-*d*]pyrimidin-4(5*H*)-one **(14)**. Yield: 89%. MP: > 300 °C. IR (cm^{-1}): 3113; 1724; 1597; 1510; 1233. ^{1}H NMR (400 MHz, DMSO-d_6, TMS, δ in ppm): 7.44-7.40 (m; 2H; H3', H5'); 8.08-8.04 (m; 2H; H2', H6'); 8.21 (d; 1H; H6; J = 3.8 Hz); 8.33 (s; 1H; H3); 12.47 (s; 1H; OH). ^{13}C NMR (100 MHz, DMSO-d_6, TMS, δ in ppm): 107.5 (C3a); 116.1 (d; J = 22.9 Hz; C3', C5'); 123.8 (d; J = 8.6 Hz; C2', C6'); 134.6 (d; J = 2.7 Hz; C1'); 136.0 (C3); 148.9 (C6); 157.1 (C4); 151.7 (C7a); 160.6 (d; J = 242.8 Hz; C4'). ^{19}F NMR (376 MHz, DMSO-d_6, TMS, δ in ppm): -114.88. EI $[M+1]^+$ 231.07.

1-(4-chlorophenyl)-1*H*-pyrazolo[3,4-*d*]pyrimidin-4(5*H*)-one **(15)**. Yield: 73%. MP: > 300 °C. IR (cm^{-1}): 3097; 1795; 1667; 1597; 824. ^{1}H NMR (400 MHz, DMSO-d_6, TMS, δ in ppm): 7.66 (d; 2H; J = 6.8 Hz; H3', H5'); 8.13 (d; 2H; J = 6.8 Hz ; H2', H6'); 8,22 (d; 1H; J = 3.8 Hz; H6); 8.36 (s; 1H; H3); 12.51 (s; 1H; OH). ^{13}C NMR (100 MHz, DMSO-d_6, TMS, δ in ppm): 107.7 (C3a); 123.0 (C2', C6'); 129.2 (C3', C5'); 131.2 (C4'); 136.3 (C3); 137.1 (C1'); 149.0 (C6); 151.9 (C7a); 157.1 (C4). EI $[M+1]^+$ 247.07.

1-(*p*-tolyl)-1*H*-pyrazolo[3,4-*d*]pyrimidin-4(5*H*)-one **(16)**. Yield: 80%. MP: 275–277 °C. IR (cm^{-1}): 3094; 1667; 1589; 1510; 1397. ^{1}H NMR (400 MHz, DMSO-d_6, TMS, δ in ppm): 2.37 (s; 3H; CH_3); 7.36 (d; 2H; J = 8.4 Hz; H3', H5'); 7.91 (d; 2H; J = 8.4 Hz; H2', H6'); 8.18 (s; 1H; H6); 8.30 (s; 1H; H3); 12.42 (s; 1H; OH). ^{13}C NMR (100 MHz, DMSO-d_6, TMS, δ in ppm): 20.5 (CH_3); 107.4 (C3a); 121.6 (C2', C6'); 129.5 (C3', C5'); 135.7 (C4'); 135.8 (C3); 136.5 (C1'); 148.6 (C6); 151.6 (C7a); 157.2 (C4). EI $[M+1]^+$ 227,07.

1-(4-cyanophenyl)-1*H*-pyrazolo[3,4-*d*]pyrimidin-4(5*H*)-one **(17)**. Yield: 68%. MP: > 300 °C. IR (cm^{-1}): 3111-3004; 2950-2884; 2231; 1717; 1595; 1535. ^{1}H NMR (400 MHz, DMSO-d_6, TMS, δ in ppm): 8.06 (d; 2H; J = 8.9 Hz; H3', H5'); 8.28 (d; 1H; H6); 8.38 (d; 2H; J = 8.9 Hz; H2', H6'); 8.44 (s; 1H; H3); 12.63 (s; 1H; NH). ^{13}C NMR (100 MHz, DMSO-d_6, TMS, δ in ppm): 108.2 (C3a); 108.9 (C4'); 118.3 (CN); 121.2 (C2', C6'); 133.6 (C3', C5'); 137.2 (C3); 141.6 (C1'); 149.4 (C6); 152,6 (C7a); 156.9 (C4). EI $[M+1]^-$ 236.07.

1-(4-(trifluoromethyl)phenyl)-1*H*-pyrazolo[3,4-*d*]pyrimidin-4(5*H*)-one **(18)**. Yield: 83%. MP: > 300 °C. IR (cm^{-1}): 3101-3018; 1671; 1540; 1593; 1319. ^{1}H NMR (400 MHz, DMSO-d_6, TMS, δ in ppm): 7.96 (d; 2H; J = 8.7 Hz; H3', H5'); 8.28 (d; 1H; H6); 8.38 (d; 2H; J = 8.7 Hz; H2', H6'); 8.42 (s; 1H; H3); 12.60 (s; 1H; NH). ^{13}C NMR (100 MHz, DMSO-d_6, TMS, δ in ppm): 108.2 (C3a); 121.4 (C2', C6'); 124.0 (q; J = 270.4 Hz; CF_3); 126.9 (q; J = 32.0 Hz; C4'); 126.9 (q; J = 3.9 Hz; C3', C5'); 136.9 (C3); 141.4 (C1'); 149.4 (C6); 152.5 (C7a); 157.0 (C4). ^{19}F NMR (376 MHz, DMSO-d_6, TMS, δ in ppm): -60.79. EI $[M+1]^-$ 279.10.

5.1.3. General procedure for preparing 4-chloro-1-phenyl-1*H*-pyrazolo[3,4-*d*]pyrimidines (19-24)

To 0.004 mol of derivatives **13-18** was added 10 mL of phosphorus oxychloride. The mixture stirred under reflux for 24 h. Excess solvent was removed under reduced pressure, and the resulting material was carefully added to 50 mL of crushed ice. The mixture was then basified to pH 7 with aqueous NaOH (6 M) and stirred for 40 min. The mixture was diluted with water (30 mL) and extracted with chloroform (3 × 30 mL). The combined organic solution was washed with water (3 × 50 mL), dried over anhydrous sodium sulfate, filtered, and concentrated under vacuum to produce **19-24** in 78-97% yield.

4-chloro-1-phenyl-1*H*-pyrazolo[3,4-*d*]pyrimidine **(19)**. Yield: 94%. MP: 125-126 °C. IR (cm^{-1}): 3110 (C=C-H); 1663 (C=C); 1542 (C=N); 856 (C-Cl). ^{1}H NMR (400 MHz, DMSO-d_6, TMS, δ in ppm): 8.16-7.44 (m; 5H; HAr); 8.76 (s; 1H; H3); 8.99 (s; 1H; H6). ^{13}C NMR (100 MHz, DMSO-d_6, TMS, δ in ppm): 114.6 (C3a); 121.2 (C2', C6'); 127.3 (C4'); 129.3 (C3', C5'); 133.9 (C3); 137.7 (C1'); 152.5 (C7a); 154.1 (C4). 155.3 (C6). EI $[M+1]^+$ 231.07.

4-chloro-1-(4-fluorophenyl)-1*H*-pyrazolo[3,4-*d*]pyrimidine **(20)**. Yield: 87%. MP: 158-160 °C (dg). IR (cm^{-1}): 3113; 1588; 1508; 1197; 838. ^{1}H NMR (400 MHz, DMSO-d_6, TMS, δ in ppm): 7.50-7.45 (m; 2H; H3', H5'); 8.18-8.14 (m; 2H; H2', H6'); 8.76 (s; 1H; H3); 8.98 (s; 1H; H6). ^{13}C NMR (100 MHz, DMSO-d_6, TMS, δ in ppm): 114.4 (C3a); 116.4 (d; J = 22.8 Hz; C3', C5'); 123.4 (d; J = 8.6 Hz; C2', C6'); 133.9 (C3); 134.1 (d; J = 2.8 Hz C1'); 152.4 (C7a); 154.1 (C4). 155.3 (C6); 160.6 (d; J = 243 Hz; C4'). ^{19}F NMR (376 MHz, DMSO-d_6, TMS, δ in ppm): -114.37. EI $[M+1]^+$ 249.07.

4-chloro-1-(4-chlorophenyl)-1*H*-pyrazolo[3,4-*d*]pyrimidine **(21)**. Yield: 97%. MP: 140-142°C (dg). IR (cm^{-1}): 3110; 1698; 1541; 854; 824. ^{1}H NMR (400 MHz, DMSO-d_6, TMS, δ in ppm): 7.67 (d; 2H; J = 6.8 Hz; H3', H5'); 8.19 (d; 2H; J = 6.8 Hz; H2', H6'); 8.76 (s; 1H; H3); 8.99 (s; 1H; H6). ^{13}C NMR (100 MHz, DMSO-d_6, TMS, δ in ppm): 114.7 (C3a); 122.4 (C2', C6'); 129.3 (C3', C5'); 131.3 (C4'); 134.2 (C3); 136.5 (C1'); 152.5 (C7a); 154.1 (C4). 155.4 (C6). EI $[M+1]^+$ 265.07.

4-chloro-1-(*p*-tolyl)-1*H*-pyrazolo[3,4-*d*]pyrimidine **(22)**. Yield: 78%. MP: 128-130 °C (dg). IR (cm^{-1}): 3094; 1677; 1539; 1351; 815. ^{1}H NMR (400 MHz, DMSO-d_6, TMS, δ in ppm): 2.39 (s; 3H; CH_3).7.43 (d; 2H; J = 8.4 Hz; H3', H5'); 8.02 (d; 2H; J = 8.4 Hz; H2', H6'); 8.74 (s; 1H; H3); 8.97 (s; 1H; H6). ^{13}C NMR (100 MHz, DMSO-d_6, TMS, δ in ppm): 114.4 (C3a); 121.2 (C2', C6'); 129.7 (C3', C5'); 133.6 (C3); 135.3 (C4'); 136.8 (C1'); 152.3 (C7a); 154.0 (C4). 155.2 (C6). EI $[M+1]^+$ 245.05.

4-chloro-1-(4-cyanophenyl)-1*H*-pyrazolo[3,4-*d*]pyrimidine **(23)**. Yield: 87%. MP: 185-186 °C. IR (cm^{-1}): 3107 (C=C-H); 2231 (C≡N); 1694 (C=C); 1509 (C=N); 837 (C-Cl). ^{1}H NMR (400 MHz, DMSO-d_6, TMS, δ in ppm): 8.11 (d; 2H; J = 8.9 Hz; H3', H5'); 8.47 (d; 2H; J = 8.9 Hz; H2', H6'); 8.87 (s; 1H; H3); 9.06 (s; 1H; H6). ^{13}C NMR (100 MHz, DMSO-d_6, TMS, δ in ppm): 109.1 (C3a); 115.3 (C4'); 118.3 (CN); 120.8 (C2', C6'); 133.8 (C3', C5'); 135.3 (C3); 141.2 (C1'); 153.3 (C7a); 154.3 (C4). 155.7 (C6). EI $[M+1]^+$ 255.99.

4-chloro-1-(4-(trifluoromethyl)phenyl)-1*H*-pyrazolo[3,4-*d*]pyrimidine **(24)**. Yield: 86%. MP: 89-91 °C. IR (cm^{-1}): 1582 (C=C); 1523 (C=N); 1114 (C-F); 843 (C-Cl). ^{1}H NMR (400 MHz, DMSO-d_6, TMS, δ in ppm): 7.89 (d; 2H; J = 8.6 Hz; H3', H5'); 8.56 (d; 2H; J = 9.5 Hz; H2', H6'); 8.57 (s; 1H; H3); 8.93 (s; 1H; H6). ^{13}C NMR (100 MHz, DMSO-d_6, TMS, δ in ppm): 115.1 (C3a); 120.9 (C2', C6'); 123.9 (q; J = 270.4 Hz; CF_3); 126.7 (q; J = 3.8 Hz; C3', C5'); 127.0 (q; J = 32.0 Hz; C4'); 134.9 (C3); 140.9 (C1'); 152.4 (C7a); 154.3 (C4); 155.7 (C6). ^{19}F NMR (376 MHz, DMSO-d_6, TMS, δ in ppm): -63.92.

5.1.4. General procedure for preparing 2-(1-phenyl-1*H*-pyrazolo[3,4-*d*]pyrimidin-4-yl)hydrazinecarbothioamides (1-6)

The reaction of the appropriate 4-chloro-1-phenyl-1*H*-pyrazolo[3,4-*d*]pyrimidine (**19-24**) (0.0027 mol) and 0.5 g of thiosemicarbazide (0.005 mol) in 10 mL of DMF was stirred at 25 °C for 24 h and was then poured into ice cold water (50 mL). The precipitate was collected by filtration and washed with water and dried. The residual crude product was recrystallized from ethanol/water (3:1). Compounds **1-6** were obtained in 23-50% yield.

2-(1-phenyl-1*H*-pyrazolo[3,4-*d*]pyrimidin-4-yl)hydrazinecarbothioamide **(1)**. Yield: 50%. MP: 190-192 °C. IR (cm^{-1}): 3433 (NH_2); 3153 (NH); 1426-1236 (C=S); 1288 (C-N). ^1H NMR (400 MHz, DMSO-d_6, TMS, δ in ppm): 7.39-7.35 (m; 1H; H4'); 7.59-7.55 (m; 2H; H3', H5'); 7.91 (s; 1H; NH'); 8.18 (d; 3H; J = 7.7 Hz; H2', H6'); 8.18 (d; 3H; H3); 8.28 (s; 1H; NH''); 8.47 (s; 1H; H6); 10.16 (s; 2H; NH_2). ^{13}C NMR (100 MHz, DMSO-d_6, TMS, δ in ppm): 100.2 (C3a); 120.8 (C2', C6'); 126.3 (C4'); 129.1 (C3', C5'); 134.0 (C3); 138.4 (C1'); 153.5 (C7a); 155.7 (C6); 159.6 (C4); 182.2 (C=S). HRMS (ESI) calc. for $C_{12}H_{11}N_7S$ 285.0797; found $[M-1]^-$ 284.0736. HPLC: 97.7%.

2-(1-(4-fluorophenyl)-1*H*-pyrazolo[3,4-*d*]pyrimidin-4-yl)hydrazinecarbothioamide **(2)**. Yield: 27%. MP: 274-276 °C. IR (cm^{-1}): 3225 (NH_2); 3058 (NH); 1426-1048 (C=S); 1286 (C-N). ^1H NMR (400 MHz, DMSO-d_6, TMS, δ in ppm): 7.45-7.39 (m; 2H; H3', H5'); 7.91 (s; 1H; NH'); 8.22-8.17 (m; 3H; H2', H6'); 8.22-8.17 (m; 3H; H3); 8.27 (s; 1H; NH''); 8.46 (s; 1H; H6); 10.17 (d; 2H; NH_2). ^{13}C NMR (100 MHz, DMSO-d_6, TMS, δ in ppm): 100.1 (C3a); 115.9 (d; J = 22.6 Hz; C3', C5'); 122.8 (d; J = 7.8 Hz; C2', C6'); 134.0 (C1'); 134.8 (C3); 153.4 (C7a); 155.8 (C6); 159.6 (C4); 160.0 (d; J = 242.0 Hz; C4'); 182.2 (C=S). ^{19}F NMR (376 MHz, DMSO-d_6, TMS, δ in ppm): -115.73. HRMS (ESI) calc. for $C_{12}H_{10}FN_7S$ 303.0702; found $[M+1]^+$ 304.0788. HPLC: 98.7%.

2-(1-(4-chlorophenyl)-1*H*-pyrazolo[3,4-*d*]pyrimidin-4-yl)hydrazinecarbothioamide **(3)**. Yield: 25%. MP: 278-279 °C. IR (cm^{-1}): 3094 (NH); 1433-1071 (C=S); 1282 (C-N). ^1H NMR (400 MHz, DMSO-d_6, TMS, δ in ppm): 7.64 (d; 2H; J = 8.9 Hz; H3', H5'); 7.92 (s; 1H; NH'); 8.21 (s; 1H; NH''); 8.26 (d; 2H; J = 8.9 Hz; H2', H6'); 8.27 (s; 1H; H3); 8.49 (s; 1H; H6); 10.19 (d; 2H; NH_2). ^{13}C NMR (100 MHz, DMSO-d_6, TMS, δ in ppm): 100.3 (C3a); 122.1 (C2', C6'); 129.1 (C3', C5'); 130.3 (C4'); 134.4 (C1'); 137.3 (C3); 153.7 (C7a); 155.9 (C6); 159.7 (C4); 182.3 (C=S). HRMS (ESI) calc. for $C_{12}H_{10}ClN_7S$ 319.0407; found $[M+1]^+$ 320.0492. HPLC: 93.2%.

2-(1-(p-tolyl)-1*H*-pyrazolo[3,4-*d*]pyrimidin-4-yl)hydrazinecarbothioamide **(4)**. Yield: 23%. MP: 264-266 °C. IR (cm^{-1}): 3389 (NH_2); 3268, 3124 (NH); 1433-1075 (C=S); 1284 (C-N). ^1H NMR (400 MHz, DMSO-d_6, TMS, δ in ppm): 2.37 (s; 3H; CH_3); 7.36 (d; 2H; J = 8.2 Hz; H3', H5'); 7.89 (s; 1H; NH'); 8.04 (d; 2H; J = 8.5 Hz; H2', H6'); 8.18 (s; 1H; H3); 8.25 (s; 1H; NH''); 8.45 (s; 1H; H6); 10.14 (d; 2H; NH_2). ^{13}C NMR (100 MHz, DMSO-d_6, TMS, δ in ppm): 20.4 (CH_3); 100.1 (C3a); 120.7 (C2', C6'); 129.4 (C3', C5'); 131.7 (C4'); 135.6 (C3); 136.1 (C1'); 153.3 (C7a); 155.6 (C6); 159.6 (C4); 182.2 (C=S). HRMS (ESI) calc. for $C_{13}H_{13}N_7S$ 299.0953; found $[M+1]^+$ 300.1025. HPLC: 88.5%.

2-(1-(4-cyanophenyl)-1*H*-pyrazolo[3,4-*d*]pyrimidin-4-yl)hydrazinecarbothioamide **(5)**. Yield: 28%. MP: 322-323 °C. IR (cm^{-1}): 3231 (NH_2); 3065 (NH); 2227 (C≡N); 1407-1051 (C=S); 1284 (C-N). ^1H NMR (400 MHz, DMSO-d_6, TMS, δ in ppm): 7.95 (s; 1H; NH'); 8.05 (d; 2H; J = 8.9 Hz; H3', H5'); 8.23 (s; 1H; NH''); 8.34 (s; 1H; H3); 8.52 (d; 2H; J = 8.9 Hz; H2', H6'); 8.53 (s; 1H; H6); 10.24 (d; 2H; NH_2). ^{13}C NMR (100 MHz, DMSO-d_6, TMS, δ in ppm): 101,2 (C3a); 108,7 (C4'); 119,1 (CN); 120,9 (C2', C6'); 134,2 (C3', C5'); 136.0 (C3); 142.5 (C1'); 155.1 (C7a); 156.7 (C6); 160.3 (C4); 182.7 (C=S). HRMS (ESI) calc. for $C_{13}H_{10}N_8S$ 310.0749; found $[M+1]^+$ 311.0829. HPLC: 94.6%.

2-(1-(4-(trifluoromethyl)phenyl)-1*H*-pyrazolo[3,4-*d*]pyrimidin-4-yl)hydrazinecarbothioamide **(6)**. Yield: 25%. MP: 282-284 °C. IR (cm^{-1}): 3413 (NH_2); 3265; 3095 (NH); 1438-1061 (C=S); 1319 (C-F); 1288 (C-N). ^1H NMR (400 MHz, DMSO-d_6, TMS, δ in ppm): 7.84 (d; 2H; J = 8.6 Hz; H3', H5'); 8.41 (s; 1H; H3); 8.47 (s; 1H; H6); 8.51 (d; 2H; J = 8.6 Hz; H2', H6'). ^{13}C NMR (100 MHz, DMSO-d_6, TMS, δ in ppm): 102.5 (C3a); 122.3 (s; C2', C6'); 125.6 (q; CF_3; J = 269 Hz); 127.4 (q; C3', C5'; J = 3.7 Hz); 127.4 (C3); 129.2 (q; C4'; J = 32.4 Hz); 136.1 (C1'); 143.3 (C7a); 155.9 (C4); 157.1 (C6); 184.9 (C=S). HRMS (ESI) calc. for $C_{13}H_{10}F_3N_7S$ 353.0670; found $[M-1]^-$ 354.0757. HPLC: 100.0%.

5.2. Biological evaluation

5.2.1. Kinetics of arginase inhibition

Arginase inhibition was performed using recombinant enzyme from *L. amazonensis* produced in *E. coli* and purified as described previously.[8] The inhibition trial was performed using 50 mM L-arginine in 50 mM CHES buffer, pH 9.5, and 100 µM of each compound in triplicate in two independent experiments. The compounds were diluted first in DMSO at 70 mM and before the inhibition assays, all were diluted at 1 mM in deionized water. The compounds that showed inhibition greater than 70% at 100 µM were used to determine the IC_{50}, Ki and mechanism of inhibition. The IC_{50} determination was performed with three concentrations of L-arginine substrate (25 mM, 50 mM and 100 mM) separately in triplicate in two independent experiments using concentrations varying from 200 to 0.05 µM obtained by a 4-fold serial dilution. The data were analyzed by nonlinear regression using a sigmoidal model (logDose × enzyme activity) using GraphPad Prisma 7.0.[29] The kinetics were performed using three concentrations of substrate and three concentrations of each inhibitor. The data were analyzed graphically using Dixon[30] and Cornish-Bowden[31] plots using a linear regression model and MS-Excel. The dissociation constant Kis was calculated by the intersection point found between the lines with different slopes[29] on a Cornish-Bowden plot.

5.2.2. Anti-leishmanicidal *in vitro* assay

Animals: Male Swiss Webster mice (18-20 g) were obtained from the animal facilities of ICTB (Institute of Science and Biomodels Technology/Fiocruz/RJ/Brazil). Animals were housed in a maximum of 6 per cage, kept in a specific-pathogen-free (SPF) room at 20 to 24 °C under a 12 h light and 12 h dark cycle, providing sterilized water and chow ad libitum. All mice were allowed acclimate for 7 days before starting the experiments.

Parasites: Amastigotes from *L. amazonensis* (LTB0016) were obtained from the skin lesions of posterior paws of Swiss Webster male mice infected (subcutaneously) with 10^6 amastigotes/per mouse. At the 30 days post infection, the skin lesions were aseptically removed and the parasite purified following mechanical dissociation using RPMI medium as reported.[32]

Compound screening *in vitro*: The effect of the studied compounds against the amastigotes was evaluated using the following protocol: parasites (10^6/well in 96-well microplates) were incubated for 48 h at 32 ºC in an atmosphere of 5% CO_2 in the presence or not of the tested compounds up to 30 µM. After 48 h of compound incubation, the samples were incubated for 24 h at 32 °C with 10% AlamarBlue (Invitrogen) solution and then the O.D read at 570-600 nm following the manufacturer's instructions. Pentamidine was used in parallel as the reference drug. Stock compound solutions (20 mM) were dissolved in DMSO (dimethylsulfoxide) and fresh dilutions were prepared extemporaneously, with the final concentration never exceeding 0.6% for *in vitro* experiments.[33]

5.2.3. Cytotoxicity assays

Cytotoxicity assays using mammalian host cells: The toxic aspects of each compound on mammalian cells was performed by using primary cultures of peritoneal macrophages obtained from Swiss male mice (18-20 g) previously inoculated with 1 mL 3% thioglycolate. After 96 h of thioglycolate stimulation, the peritoneal cells were harvested by rinsing the animals' peritoneum with RPMI 1-640. The peritoneal cells were then plated into 96-well microplates at a cell density of 10^5 cells/well as reported.[34] The cultures were then sustained in RPMI 1640 medium (pH 7.2 to 7.4) without phenol red (Gibco BRL) supplemented with 10% fetal bovine serum and 2 mM glutamine.[33] After 24 h of platting, the compounds (up to 200 µM) were added and the cultures incubated for 48 h at 37 ºC in an atmosphere of 5% CO_2 and air. Then, MTT solution was added to the treated cultures (0.45 mg/mL), and after 4 h of incubation, the O.D. read at 570 nM by a UV spectrophotometer. The results were calculated according to the manufacturer's instructions and the concentration that reduced host cell viability by 50% (LC_{50}) calculated. All assays were run at least 2 times in triplicate.[34] Ethics: All procedures were carried out in accordance with the guidelines established by the FIOCRUZ Committee of Ethics for the Use of Animals (CEUA LW16/14).

5.3. Molecular Modeling

5.3.1. Comparative modeling

The amino acid sequence of *L. amazonensis* arginase (*La*ARG, UniProtKB ID: O96394) was obtained from the ExPASy server.[35] The region between Glu12-Thr318, the portion of the LaARG sequence that includes the whole catalytic core, was considered to construct the models in monomeric and trimeric forms, using the MODELLER v9.19 program (http://salilab.org/modeler/) and crystal structures 1T5G and 4ITY as templates.[24] Subsequently, the models were refined using the same program. Thus, the final models were validated using two programs: PROCHECK and VERIFY3D.[21,22] PROCHECK analyzes the stereochemical quality and VERIFY3D performs compatibility analysis between the 3D model and its own amino acid sequence by assigning a structural class based on its location and environment, and by comparing the results with crystal structures with good resolution.[21,22]

5.3.2. Molecular Docking

The inhibitor structures (1 and 6) were built suing Spartan'14 software (Wavefunction, Inc., Irvine, CA). The docking of the two inhibitors into the monomeric and trimeric LaARG models were performed using the Molegro Virtual Docker 6.0 (MVD) program (CLC bio, Aarhus, Denmark),[26] which uses a heuristic search algorithm that combines differential evolution with a cavity prediction algorithm. The MolDock scoring function used is based on a modified piecewise linear potential (PLP) with new hydrogen bonding and electrostatic terms included. A full description of the algorithm and its reliability compared to other common docking algorithms has been described.[26] As no satisfactory cavities were found by the cavity prediction algorithm using MVD, the whole enzyme, in the monomeric form, and the whole three chains of the enzymes, in the trimeric form, were set as the center of the searching space. The search algorithm MolDock optimizer was used with a minimum of 100 runs, and the parameter settings were: population size = 500; maximum iteration = 2000; scaling factor = 0.50; offspring scheme = Scheme 1; termination scheme = variance-based; crossover rate = 0.90. Due to the stochastic nature of the algorithm search, ten independent simulations per ligand were performed to predict the binding mode. Consequently, the complexes with the lowest interaction energy were evaluated. The interactions between LaARG, in both forms, and each inhibitor were analyzed using the ligand map algorithm, a standard algorithm in the MVD program.[26] The usual threshold values for H-bonds and steric interactions were used. All figures for LaARG modeling and molecular docking results were edited using the Visual Molecular Dynamics 1.9.3 (VMD) program (available for download at http://www.ks.uiuc.edu/Research/vmd/vmd-1.9.3/).

Acknowledgments

This study was financed in part by the Coordenacao de Aperfeiçoamento de Pessoal de Nivel Superior - Brasil (CAPES) - Finance Code 001. The authors thank the Coordination of Superior Level Staff Improvement (CAPES) and the National Council of R&D of Brazil (CNPq) for the fellowships granted to the authors. JAASSC is a fellowship of Ministério da Ciência e Tecnologia Ensino Superior e Técnico-Profissional de Moçambique (MCTESTP). We also thank the Foundation for Research of the State of Rio de Janeiro (FAPERJ), Technological Development Program on Products for Health (PDTIS) and São Paulo Research Foundation (FAPESP, #17/06917-4) for financial support. ERS, NB, MNCS, and LCSP are recipient of research productivity fellowships from the CNPq and NB and MNCS thank the ("Cientista do Nosso Estado") from FAPERJ.

References and notes

1. World Health Organization (WHO). Leishmaniasis. Available at: http://www.who.int/leishmaniasis/en/ Accessed: 14/01/2019.
2. Croft, S. L.; Yardley, V. *Curr. Pharm. Des.* **2002**, *8*, 319–342.
3. Aronson, N.; Herwaldt, B. L.; Libman, M.; Pearson, R.; Lopez-Velez, R.; Weina, P.; Carvalho, E.; Ephros, M.; Jeronimo, S.; Magill, A. *Clin. Infect. Dis.* **2016**, *63*, 1539–1557.
4. Boechat, N.; Pinheiro, L. C. S. *An Overview of New Synthetic Antileishmanial Candidates*, 2014, 63-121. In Adilson Beatriz and Dênis Pires de Lima (Eds) *Organic Compounds to Combat Neglected Tropical Diseases* Chapter 3 Bentham Science Publishers **2014**.
5. Fairlamb, A. H.; Cerami, A. *Annu. Rev. Microbiol*. **1992**, *46*, 695–729.
6. Mukbel, R. M.; Patten, C. Jr.; Gibson, K.; Ghosh, M.; Petersen. C.; Jones, D. E. *Am. J. Trop. Med. Hyg.* **2007**, *76*, 669–675.
7. Bocedi, A.; Dawood, K. F.; Fabrini, R.; Federici, G.; Gradoni, L.; Pedersen, J. Z.; Ricci, G. *FASEB J.*, **2010**, *24*, 1035–1042.
8. Da Silva, E. R.; Da Silva, M. F.; Fischer, H.; Mortara, R. A.; Mayer, M. G.; Framesqui, K.; Silber, A. M.; Floeter-Winter, L. M. *Mol. Biochem. Parasitol.* **2008**, *159*, 104–11.
9. Riley, E.; Roberts, S. C.; Ullman, B. *Int. J. Parasitol.* **2011**, *41*, 545–552.
10. Iniesta, V.; Gómez-Nieto, L. C.; Corraliza, I. *J. Exp. Med.* **2001**, *193*, 777–784.
11. D'Antonio, E. L.; Ullman, B.; Roberts, S. C.; Dixit, U. G.; Wilson, M. E.; Hai, Y.; Christianson, D. W. *Arch. Biochem. Biophys.* **2013**, *535*, 163–176.
12. Baggio, R.; Elbaum, D.; Kanyo, Z. F.; Carroll, P. J.; Cavalli, R.; Ash, D. E.; Christianson, D. W. *J. Am. Chem. Soc.* **1997**, *119*, 8107–8108.
13. Kim, N. N.; Cox, J. D.; Baggio. R. F.; Emig, F. A.; Mistry, S. K.; Harper, S. L.; Speicher, D. W.; Morris, S. M. Jr; Ash, D. E.; Traish, A.; Christianson, D. W. *Biochemistry.* **2001**, *40*, 2678–88.
14. Boechat, N.; Pinheiro, L. C. S.; Silva, T. S.; Aguiar, A. C. C.; Carvalho, A. S.; Bastos, M. M.; Costa, C. C. P.; Pinheiro, S.; Pinto, A. C.; Mendonça, J. S.; Dutra, K. D. B.; Valverde, A. L.; Santos-Filho, O. A.; Ceravolo, I. P.; Krettli, A. U. *Molecules.* **2012**, *17*, 8285–8302.
15. Boechat. N.; Lages, A. S.; Santos-Filho, O. A.; Genestra, M.; Bastos, M. M.; Kover, W. B. *J. Microbiol. Antimicrob.* **2013**, *5*, 72–86.
16. Da Silva, E. R.; Boechat, N.; Pinheiro, L. C. S.; Bastos, M. M.; Costa, C. C.; Bartholomeu, J. C.; da Costa, T. H. *Chem. Biol. Drug Des.* **2015**, *86*, 969–978.

17. Dos Santos, M. S.; Bernardino, A. M. R.; Pinheiro, L. C. S.; Marilene, M.; Canto-Cavalheiro, M. M.; Leon, L. L. *J. Heterocyclic Chem.* **2012**, *49*, 1425–1428.
18. Silveira, F. F.; Feitosa, L. M.; Mafra, J. C. M.; Ferreira, M. L. G.; Rogerio, K. R.; Carvalho, L. J. M.; Boechat, N.; Pinheiro, L. C. S. *Med. Chem. Res.* **2018**, *27*, 1876–1884.
19. Silva, T. B.; Bernardino, A. M. R.; Ferreira, M. L. G.; Rogerio, K. R.; Carvalho, L. J. M.; Boechat, N.; Pinheiro, L. C. S. *Bioorg. Med. Chem.* **2016**, *24*, 4492–4498.
20. Pinheiro, L. C.; Boechat, N.; Ferreira, M. L. G.; Júnior, C. C.; Jesus, A. M.; Leite, M. M.; Souza, N. B.; Krettli, A. U. *Bioorg. Med. Chem.* **2015***, 23*, 5979–5984.
21. Laskowski, R. A.; MacArthur, M. W.; Moss, D. S.; Thornton, J. M. *J. Appl. Cryst.* **1993**, *26*, 283–291.
22. Eisenberg, D.; Lüthy, R.; Bowie, Ju. VERIFY3D: Assessment of protein models with three-dimensional profiles. *Methods in enzymology* **1997**, *277*, 396–404. In: Charles W. Carter Jr., Robert M. Sweet (Eds) Macromolecular Crystallography Part B. Elsevier Publishers 1997.
23. Caldwell, R. B.; Toque, H. A.; Narayanan, S. P.; Caldwell, R. W. *Trends Pharmacol. Sci.* **2015**, *36*, 395–405.
24. Ash, D. E *J. Nutr.* **2004**, *134*, 2760S–2764S.
25. Cama, E.; Pethe, S.; Boucher, J. L.; Han, S.; Emig, F. A.; Ash, D. E.; Viola, R. E.; Mansuy, D.; Christianson, D. W. *Biochemistry.* **2004**, *43*, 8987–8999.
26. Thomsen, R.; Christensen, M. H. *J. Med. Chem.* **2006**, *49*, 3315–3321.
27. Lavulo, L. T.; Sossong, T. M. Jr, Brigham-Burke, M. R.; Doyle, M. L.; Cox, J. D.; Christianson, D. W.; Ash, D. E. *J. Biol. Chem.* **2001**, *276*, 14242–14248.
28. Da Silva, E. R.; Maquiaveli, C. C.; Magalhães, P. P. *Exp. Parasitol.* **2012**, *130*, 183–188.
29. Dos Reis, M. B. G.; Manjolin, L. C.; Maquiaveli, C. C.; Santos-Filho, O. A.; Da Silva, E. R. *PLoS One.* **2013**, *8*, e78387.
30. Dixon; M. *Biochem. J.* **1953**, *55*, 170-171.
31. Cornish-Bowden, A. *Biochem. J.* **1974**, *137*, 143–144.
32. De Souza, E. M.; Lansiaux, A.; Bailly, C.; Wilson, W. D.; Hu, Q.; Boykin, D. W.; Batista, M. M.; Araújo-Jorge, T. C.; Soeiro, M. N. *Biochem. Pharmacol.* **2004**, *68*, 593–600.
33. Romanha, A. J.; Castro, S. L.; Soeiro, M. N.; Lannes-Vieira, J.; Ribeiro, I.; Talvani, A.; Bourdin, B.; Blum, B.; Olivieri, B.; Zani, C.; Spadafora, C.; Chiari ,E.; Chatelain, E.; Chaves, G.; Calzada, J. E.; Bustamante, J. M.; Freitas-Junior, L. H.; Romero, L. I.; Bahia, M. T.; Lotrowska, M.; Soares, M.; Andrade, S. G.; Armstrong, T.; Degrave, W.; Andrade, Z. A. *Mem. Inst. Oswaldo Cruz.* **2010**, *105*, 233–238.
34. Silva, C. F.; Batista, M. M.; Mota, R. A.; De Souza. E. M.; Stephens, C. E.; Som, P.; Boykin, D. W.; Soeiro, M. N. *Biochem. Pharmacol.* **2007**, *73*, 1939–1946.
35. Gasteiger, E.; Gattiker, A.; Hoogland, C.; Ivanyi, I.; Appel, R. D.; Bairoch, A. *Nucleic Acids Res.* **2003**, *31*, 3784–3788.

Graphical Abstract

.

New pyrazolopyrimidine derivatives as *Leishmania amazonensis* arginase inhibitors

Leave this area blank for abstract info.

Livia M. Feitosa[a,b], Edson R. da Silva[c,*], Lucas V. B. Hoelz[a], Danielle L. Souza[a], Julio A. A. S. S. Come[d], Camila Cardoso-Santos[e], Marcos M. Batista[e], Maria de Nazare C. Soeiro[e], Nubia Boechat[a,*] and Luiz C. S. Pinheiro[a]

[a]*Departamento de Sintese de Farmacos, Instituto de Tecnologia em Farmacos, Farmanguinhos - FIOCRUZ, Fundação Oswaldo Cruz. Rua Sizenando Nabuco 100, Manguinhos, Rio de Janeiro, RJ, 21041-250, Brazil.*

[b]*Programa de Pos-graduação em Quimica, PGQu Instituto de Quimica, Universidade Federal do Rio de Janeiro, Rio de Janeiro, RJ, Brazil.*

[c]*Departamento de Medicina Veterinaria, Faculdade de Zootecnia e Engenharia de Alimentos, Universidade de Sao Paulo, Pirassununga, SP, 13635-900, Brazil.*

[d]*Programa de Pos-graduação em Biociencia Animal, Faculdade de Zootecnia e Engenahria de alimentos, Universidade de São Paulo, Pirassununga, SP, Brazil.*

[e]*Laboratoório de Biologia Celular, Instituto Oswaldo Cruz, IOC - FIOCRUZ, Fundacao Oswaldo Cruz. Avenida Brasil 4365, Manguinhos, Rio de Janeiro, RJ, 21045-900, Brazil.*

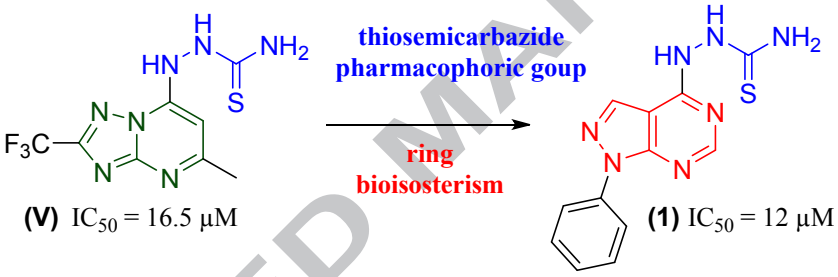

(V) IC_{50} = 16.5 µM

(1) IC_{50} = 12 µM

Highlights

- Six 1-phenyl-1*H*-pyrazolo[3,4-*d*]pyrimidine derivatives with different substituents were synthesized.
- Two compounds, **1** (R = H) and **6** (R = CF_3), showed arginase inhibition >70% and IC_{50} values of 12 μM and 55 μM, respectively.
- The molecular docking studies proposed that these two uncompetitive inhibitors interact with different *La*ARG binding sites.
- The pyrazolopyridine system system can be promising for the design of potential antileishmanial compounds.